J. Guadagnini, G. De Zaiacomo
Multidisciplinary Modeling for Missionisation of Re-Entry Vehicles
in: AIAA Scitech 2023 Forum, AIAA, 2023, ISBN: 9781624106996, p. 1-23, AIAA 2023-1169
[AIAA Scitech 2023 Forum, National Harbor, MD, USA & Online, 23-27 Jan. 2023]
doi:10.2514/6.2023-1169

Multidisciplinary Modeling for Missionisation of Re-entry Vehicles

Jacopo Guadagnini * † and Gabriele De Zaiacomo‡
Deimos Space SLU, Tres Cantos, Madrid, Spain, 28760

This work is part of the European H2020 ASCenSIon program. In this context, the global objective of this research is the definition and the development of a Mission Analysis and GNC missionisation tool for autonomous re-entry vehicles. Within ASCenSIon, missionisation has two scopes: the first concerns with the optimal adaptation of the solution for a specific mission, the second one addresses to evaluate the mission capabilties of a vehicle by means of Multidisciplinary Design Optimization (MDO). The focus of the paper is on the engineering modeling of the building blocks of the Multidisciplinary Design Analysis (MDA) framework, with the goal of identifying the disciplines and the design parameters needed to obtain robust re-entry trajectories. The design of a re-entry mission is, in fact, a multidisciplinary and complex scenario, which must take into account a broad set of Mission and System requirements. For this reason, an MDA environment with appropriate mathematical models of the problem has been developed to assess the mission performance with respect to the key design parameters. This paper gives an overview of the architecture of the tool, with particular attention on the implementation of the disciplines and their interactions, and presents an overview on MDO methodologies for solving the problem.

I. Nomenclature

Greek Symbols

α	Angle-of-attack [º]
δ	Aerodynamic surface deflection [º]
γ	Flight-Path-Angle [º]
μ	Standard gravitational parameter [m^3/s^2]
ψ	Heading angle [º]
ρ	Atmospheric Density [kg/m^3]
ρ_h	Density derivative @ altitude [kg/m^4]
σ	Bank angle [º]
$\dot{\sigma}$	Bank angle rate [º]

Roman Symbols

b	Wing span [m]
c	Mean aerodynamic chord [m]
C_0	Heat flux constant [$kg^{0.5}s^{0.15}/m^{1.15}$]
C_A	Axial aerodynamic coefficient [-]
C_D	Drag aerodynamic coefficient [-]
C_L	Lift aerodynamic coefficient [-]
C_m	Pitching moment aerodynamic coefficient [-]
C_N	Normal aerodynamic coefficient [-]
C_j	Configuration Parameter of j discipline [-]
D	Drag acceleration [m/s^2]
D'	Drag derivative @ Energy [1/m]
E	Total specific energy [m^2/s^2]
g_0	Earth gravitational acceleration at sea level [m/s^2]
g	Earth gravitational acceleration [m/s^2]
h	Altitude with respect Planet surface [m]
J	Cost function [-]
L	Lift acceleration [m/s^2]
L/D	Lift-to-Drag ratio [-]
L_{ref}	Reference Length of the vehicle [m]
m	Mass of the vehicle [kg]
m_{av}	Mass of the avionics [kg]
m_{dry}	Dry mass of the vehicle [kg]
m_{el}	Mass of the electric and power system [kg]
m_{eq}	Mass of the equipment [kg]
m_{fus}	Mass of the fuselage [kg]
m_{gear}	Mass of the landing gear [kg]
m_{hyd}	Mass of the hydraulic system [kg]
m_{pay}	Mass of the payload [kg]
m_{prop}	Mass of the propulsive system [kg]
m_{TPS}	Mass of the TPS [kg]
m_w	Mass of the wing [kg]
Ma	Mach number [-]

*PhD, Atmospheric Flight Competence Center, Deimos Space SLU, jacopo.guadagnini@deimos-space.com
†PhD, Department of Aerospace Science and Technology, Politecnico di Milano, jacopo.guadagnini@polimi.it
‡Head of Atmospheric Fligth Competence Center, Atmospheric Flight Competence Center, Deimos Space SLU, gabriele.dezaiacomo@deimos-space.com

$Diam$	Diameter of the vehicle [m]	n_g	g-load [-]
N_α	α discretization points for FQA [-]	T	Thrust [N]
N_{Ma}	Ma discretization points for FQA [-]	V	Velocity [m/s]
P	Pressure [Pa]	X_{cog}	X position of the center of gravity [m]
P_j	System and mission parameters of discipline j [-]	ΔX_{cog}	X shift-position of the center of gravity [m]
$\dot{q}_{heat}$	Heat flux at stagnation point [W/m^2]	X_j	Design variables for discipline j [-]
q_{dyn}	Dynamic pressure [Pa]	X_{ji}	Coupling variables for discipline j and i [-]
R_{nose}	Nose radius of the Vehicle [m]	Y_j	Output variables for discipline j [-]
r_p	Planet radius [m]	Z_{cog}	Z position of the center of gravity [m]
S_{ref}	Reference surface [m^2]	ΔZ_{cog}	Z shift-position of the center of gravity [m]
t	Time [s]		

II. Introduction

Ascension (Advancing Space Access Capabilities - Reusability and Multiple Satellite Injection) is born as an innovative training network with fifteen Early-Stage Researchers, ten beneficiaries, and fourteen partner organisations across Europe, to study the critical technologies for the development of the next generation of reusable space system. In this context, the objective of this research is the development of a Missionisation tool for re-entry vehicles.

In recent years, leading space agencies and private companies are financing the development of reusable space vehicles to lower the costs of space access and in-orbit studies. The re-flight capability, required by the reusability of a space transportation system, prompts the necessity of a Mission Analysis (MA) and GNC missionisation process and tool for autonomous re-entry vehicles which reduces the tailoring efforts required for each mission.

In literature there does not exist a clear definition of the word missionisation. The classical interpretation of missionisation is the recurrent activity to tailor the design of the solution for one particular mission. More in general, missionisation is the adaptation of the spacecraft mission to the customer's needs. This definition derives from several fields of space technologies. From the launch vehicle view point, missionisation includes those activities to be performed to adapt the space launcher to any particular launch and to demonstrate reliability of all operations. These operations involve the design of the trajectory, the system engineering analysis, the configuration management, the control of the process, and the data handling of the whole process [1]. A concept of missionisation has been found also in the mission analysis of the Space Shuttle, more in particular for the design of the trajectory from the entry point to the TAEM (Terminal Area Energy Management) interface. For each re-entry flight, the reference profile, the drag profile in this case, was adapted by tailoring the coefficients used to design the reference profile itself [2]. The common idea behind these views is the development and the update of the reference solution for a specific mission.

Within this research, the Mission Analysis (MA) and GNC missionisation of re-entry vehicles has a dual function. The first scope pursues the classical perspective, therefore addresses the tailoring and the updating of the mission analysis solution in terms of trajectory design with respect to the design parameters and the specific requirements of the mission itself. It applies to the last phases of the mission design and it aims at obtaining an optimal adaptation of the solution to the specific mission. The second objective is the computation of common feasible design space domain for multiple missions. The goal, in this case, is the evaluation of the mission capabilities of an autonomous re-entry vehicle, in order to define the set of feasible missions that the vehicle is able to perform, through the estimation of performance maps with respect to the key design parameters. This objective concerns with the first phases of the mission design. The MA and GNC missionisation has a crucial role in the reusability of a space vehicle, where multiple flights are expected, in fact the objective is the minimisation of the adaptation effort during the mission design phase by efficiently updating the MA and GNC solution and by obtaining already qualified solutions for a set of missions.

The trajectory design, the evaluation of the performance and, in general, the design of the end-to-end mission of an autonomous re-entry vehicle by taking into account a wide set of mission and system requirements, is a multidisciplinary design analysis and optimization procedure [3]. The development of a dedicated tool which includes all the disciplines to solve this problem is the main objective of this research. The first step to tackle this complex problem is to develop a MDA environment with proper mathematical models to assess the mission performance. The process, indeed, involves multiple disciplines, which allow for a numerical quantification of the related performance. Nonetheless, the identification of the disciplines is not sufficient, but a crucial step is the detection of the interactions (inputs and outputs) between them and the presence of loops. This operation is made by developing a proper Design Structure Matrix (DSM) [4], which is a methodology able to show in a single plot all the disciplines and all interactions among them. The main focus of this paper is to report the high-level architecture of the tool and to detail the engineering modelling of the

included disciplines. Particular attention is given to the interactions among them.

The developed MDA environment will be embedded in an optimization routine (MDO), in order to constitute a MA and GNC Missionisation tool for re-entry vehicles, which aims to improve the efficiency and the quality of the tailoring and the design of the solutions, by considering the coupling disciplines and the design variables. As mentioned above, the scope of the Missionisation tool is to reduce the time effort needed to obtain a missionized solution. The paper presents an overview on MDO methodologies to build an MDO framework and, eventually, to solve the optimization problem. To address this aim, an introduction of both classical approaches, such as Genetic Algorithm and Sequential Quadratic Programming, and Metamodel-based techniques is given [5, 6].

The continuous of this paper is organized as follows: Section III reports the high-level architecture of the missionisation tool and the DSM of the disciplines, in order to underline the interactions among them. In Section IV the engineering modeling of the building blocks of the MDA is presented. Section V gives an overview of the MDO methodologies to treat and to solve the problem. Section VI presents the conclusion of this paper and the future work.

III. Multidisciplinary Architecture

This section describes the High-Level architecture of the missionisation tool. It gives an overview of the the main modules, the disciplines considered, the auxiliary modules and data repository. As introduced in Section II, missionisation as a dual definition within this research and different application cases can be considered. The main cases are the following:

- **Missionised Solution (MS)**: it considers the optimal adaptation and updating of the solution for one particular mission.
- **Preliminary Mission Design (PMD)**: it refers to the evaluation of the mission performance with respect to the design parameters and mission constraints.

A. High-Level Architecture of the Tool

Figure 1 shows the High-Level architecture of the missionisation tool. The tool is constituted by three main modules: the user module, the design module and the missionisation layer. The user module has the objective to build the problem that the user wants to study. It sets-up all the parameters related to the environment, the vehicle, the boundary conditions and the cost function. A key point is the organization of the optimization variables for both the missionisation layer and the trajectory optimization discipline, if needed. Other task of this module is the selection of the type of analysis that the tool has to perform, by setting options and flags. The design variables that affect the performance of the vehicle and the solution are called missionsation parameters. This module is based on a standard structure to tackle the re-entry problem and categorize its parameters. The structure is organized in levels and sublevels. The main layer is defined as follows:

- **System**: data related to the features of the vehicle and its subsystems;
- **Mission**: data related to the specification of the mission and the environment;
- **Configuration**: data used to set-up the tool, the disciplines and the analysis case;

Each main level includes several sublevels related to the subsystems of the vehicles, and for describing the mission. Consequently, each sublevel is further subdivided to define a specific attribute. This standard definition takes part in the missionisation process to identify the parameters of the analyzed problem, and to understand which variables are invariant, variant or to be optimized in the routine. The distinction among them is the following:

- **Invariant:** Data that never change from mission to mission (for a specified vehicle and environment);
- **Variant:** Data that can change from mission to mission (for a specified vehicle and environment);
- **Optimization:** Variables that must be optimized for both the vehicle and the mission;

The user module has the secondary goal to build the structure of the data repository, in order to have a standard organization of the data for each mission and each version of the mission.

The core of the software is the design module. It is constituted by the Mission Analysis submodule, which comprehends a minimum set of disciplines to design a re-entry mission, and by the GNC submodule. As stated previously, several disciplines are taken into account for the assessment of the mission capabilities of the re-entry vehicle, as well as for the adaptation of the solution to a specific mission. The disciplines are:

- Geometry and Mass estimation (GEOM tool);
- Aerodynamic coefficients estimation tool (AEDB tool);
- Flying Qualities Analysis (FQA tool);
- Entry Corridor Analysis (EC tool);
- Footprint Evaluation (FE tool);

- Trajectory Optimization (TO tool);

It is worth to note, that among FQA and EC exists a loop, because the FQA tool can provide results to the EC tool which lead to non-flyable entry corridor, and so the FQA outcome must be updated. A particular discussion can be done for the GNC submodule. The GNC submodule is used when the adaptation of the reference mission profile is taken into account. Indeed, when the tool is used to compute the common feasible design space, the GNC is constituted by the variables that can be used to control the vehicle for example angle-of-attack, bank angle, and maximum thrust. In the case in which a new reference is generated, the GNC submodule has the following tasks:

- Translation of the reference profiles computed by the optimization into parameters that can be read by the specified GNC subsystem of the vehicle. This action is reflected into the tuning of the coefficients of the functions used to map the references.
- Evaluation of the performance of the GNC with respect to the design parameters depending on the inputs.

Especially by considering the second task, the GNC module is based on interchangeable black-box, whose performance depends on the inputs variables.

The function of tuning and optimizing the identified missionisation parameters is addressed to the missionisation layer. The missionisation layer is constituted by the MDO solver. This module aims at building the design space maps and updating the reference trajectory while maximising, or minimising, an objective function. An overview of promising methodologies that can be exploited is given in V.

The missionisation tool needs some auxiliary modules, such as libraries including several environmental and flight mechanic models, a data repository, simulators and a verification module. The data repository has the crucial task of tracking and saving the several versions of the same mission and the new missions that are studied. It is structured with a standard scheme in order to properly categorize the parameters and to make the process of setting-up the tool and comparing the result faster. As anticipated, one of the goals is, in fact, to have a common process to approach to a re-entry problem able to facilitate the identification of the optimization parameters of the analysed case. The data repository can be exploited also for initialing the optimization process both for the optimization trajectory tool and for the MDO routine, if needed.

B. Design Structure Matrix

A crucial analysis to be performed for the development of a multidisciplinary tool is the identification of the interactions between the different disciplines that constitute the tool. This operation allows to understand which are the inputs parameters that each discipline needs to perform the analysis. Moreover, it identifies the links between the disciplines and the presence of loops. The overall process may be supported by several methods, one of the most common is constituted by the Design Structure Matrix (DSM) approach, which is a method to visualize in a single chart

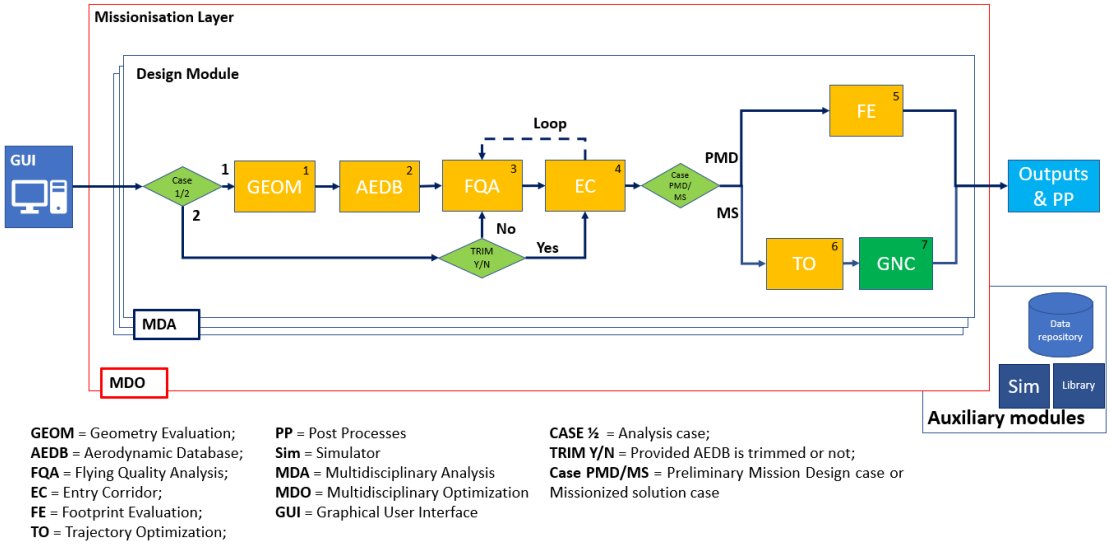

Fig. 1 High-Level architecture of the missionisation tool.

all the disciplines and the interactions among them, providing in one picture an overall view of the MDA [4]. The DSM shows in a matrix form the following information:

- Diagonal: disciplines which constitute the MDA;
- Columns: Inputs requested by a discipline and Inputs from other disciplines;
- Rows: Outputs of a discipline;

In the case in which two disciplines share both inputs and outputs, an internal loop is present and convergence is required to guarantee that coherent analyses are performed by both disciplines [3]. Figure 2 reports the DSM for the Preliminary Mission Design application case, with the concept of the vehicle variable, as an example of the multidisciplinary nature of the MA and GNC missionisation of a re-entry vehicle. This case, in fact, involves the largest set of disciplines due to the fact that the geometry, the mass and the AEDB of the vehicle are affected by the design variables and they must be estimated. The outputs of these disciplines are used for further analyses and they influence the performance of the mission. These disciplines are followed by the FQA and EC. The outputs of these last two blocks are then used to evaluate the range capabilities by the FE tool. Between FQA and EC exists a loop, due to the fact that the computation of the trim line affects the existence of a feasible entry corridor. The parameters used in the DSM are explained in Table 1. It is worth to mention that the DSM reported in this chapter is a qualitative example, especially for the specification of the parameters, but it gives an overview of the structure of the PMD problem. Moreover, the DSM can be modified depending on the problem, especially for what concerns the disciplines (for the MS case, the trajectory optimization must be considered), and optimization variables. As previously stated, the tool can be used for several problems and application cases, so slightly modifications may be performed in order to adapt the DSM to the specific case.

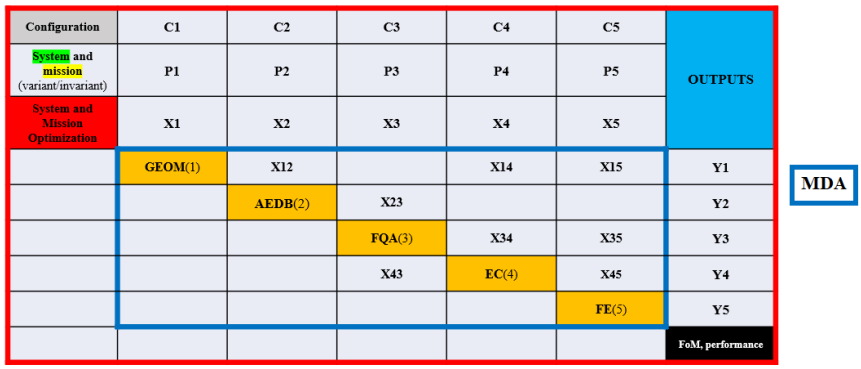

Fig. 2 Preliminary definition of Design Structure Matrix for PMD case.

Table 1 Qualitative definition of the parameters for the DSM analysis for PMD case. C_j: configuration parameters for discipline *j*; P_j: system and mission parameters (both variant and invariant) for discipline *j*; X_j: optimization variables for discipline *j*; X_{ji}: coupling variables: outputs of the discipline *j* which are inputs for discipline *i*; Y_j: outputs of the discipline *j*.

ID	Parameters	ID	Parameters	ID	Parameters
C_1	Fineness and wing-aspect ratio range	X_1	L_{ref}, Diam, b, c	X_{35}	AEDB trim
C_2	Vehicle flag	X_2	-	X_{43}	AoA trim line
C_3	AoA, Ma, deflection range and discretization points	X_3	L_{ref}, ΔX_{cog}, ΔZ_{cog}	X_{45}	Entry Corridor bounds
C_4	Atmo model, discretization points, scaling	X_4	-	Y_1	S_{ref}, mass, $\frac{L_{ref}}{\text{Diam}}$, b/c
C_5	Atmo model, discretization points, scaling, FPA0 flag	X_5	-	Y_2	C_D, C_L, C_m
P_1	AD, Structural and dynamic pressure loads	X_{12}	S_{ref}, mass, $\frac{L_{ref}}{\text{Diam}}$, b/c	Y_3	AEDB trim
P_2	AEDB function of the geometry	X_{14}	S_{ref}, mass	Y_4	Entry Corridor bounds
P_3	X_{cog}, Z_{cog}, max, min flap deflection	X_{15}	S_{ref}, mass	Y_5	Footprint
P_4	Aerothermal-mechanical laods, environment	X_{23}	C_D, C_L, C_m		
P_5	Aerothermal-mechanical laods, environment, BCs	X_{34}	AEDB trim, AoA line		

IV. Engineering Modeling of the Disciplines

This section is dedicated to the description of the disciplines included in the MDA. As mentioned within the introduction and in Section III, the missionisation of an autonomous re-entry vehicle is a multidisciplinary design analyses. The design of an end-to-end mission and the evaluation of the performance, in the context of re-entry vehicles, fall into the atmospheric flight area. Thus a minimum set of disciplines has been identified, dealing with aerodynamics, flying qualities, mission analysis, such as entry corridor and range capabilities definition, and trajectory performance. This set of disciplines constitute the core of the MDA framework: each discipline has been modelled by a mathematical model in order to numerically assess the considered performance. This section focuses on the engineering modeling of the selected disciplines, by stating the main assumptions and supplying an example of analyses. This characterization gives an overview of the key parameters of each discipline, as well as qualitatively describes the inputs and the outputs. It is worth to mention that the missionisation tool is thought to be applicable to a wide range of re-entry vehicles, from conventional lifting bodies vehicles to more novel vertical landing reusable launch vehicles. For this reason, some disciplines are specific only for some class of re-entry vehicles.

The examples reported in this section have been computed by considering the vehicle Horus-2B [7]. Its shape and design parameters are given in Figure 3 and in Table 2.

A. Geometry and Mass Estimation tool

To evaluate the performance of a re-entry vehicle, a model for the vehicle geometry and mass is required. This tool is used when the concept of the vehicle is a design variable. Typically, this can happen for the PMD application case. The geometry and mass estimation (GEOM) tool is based on several assumptions:

- The re-entry vehicles are subdivided into four main categories: Winged Re-entry Vehicles (WRV), Winged Lifting Body (WLB), Lifting Body (LB) and Vertical Landing Reusable Launcher Vehicle (VL-RLV). The tool can handle the first three categories. A detailed explanation is given in Section IV.B.
- The reference surface is computed by considering a simplified geometry of the vehicle, and it refers to the planform area.
- The position of the Center of Gravity and the Moment Reference Center coincides.
- The mass of the vehicle is estimated through a simplified version of the Hypersonic Aerospace Sizing Analysis (HASA) tool documented by [8] and [9], which is a tool based on empirical equations.

For what concerns the estimation of the dry mass of the vehicle, the tool exploits a minimum set of geometric

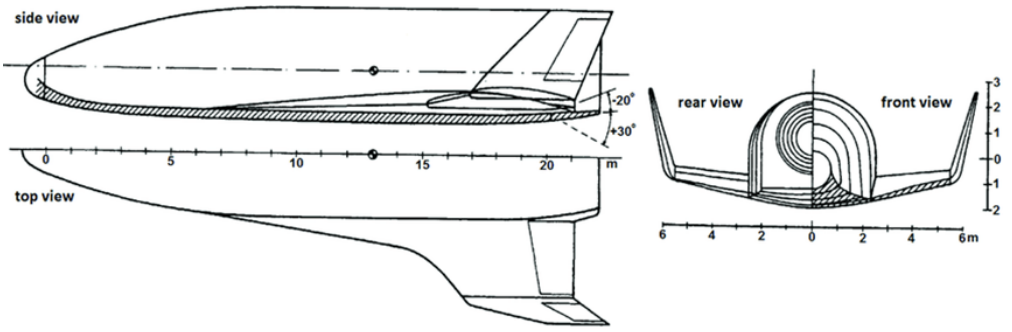

Fig. 3 Horus-2B vehicle [7].

Table 2 Horus 2-B design parameters and boundary conditions [7].

Parameter	Value	Unit			
Mass (landing configuration)	26029	kg	Max heat flux	530	kW/m^2
L/D @ hypersonic regime	1.8	-	Max axial load	2.5	-
S_{ref}	110	m^2	Flap deflection range	[-20, 30]	º
L_{ref}	23	m	Initial altitude	100	km
R_{nose}	0.8	m	Initial velocity	7.5	km/s
Max dynamic pressure	$1{\cdot}10^4$	Pa			

parameters: longitudinal length L_{ref}, diameter $Diam$, mean aerodynamic chord c and wing span b (if the vehicle is equipped with wing), and the value of the maximum dynamic pressure and mechanical load that the vehicle can withstand. Thus, the vehicle is subdivided in parts and subsystems, and the mass of each element is computed by empirical relations. The parts include the wings and the TPS, while the considered subsystems are the landing gear, the hydraulic, the avionics, the propulsive system, the electric and power system and other auxiliary equipment [8]. The dry mass is the sum of each components by considering also the payload mass (Eq. 1). Table 3 summarizes the inputs and outputs of this discipline.

$$m_{dry} = m_{pay} + m_{fus} + m_{TPS} + m_w + m_{gear} + m_{hyd} + m_{av} + m_{el} + m_{prop} + m_{eq} \tag{1}$$

The performance of the GEOM tool have been preliminary validated by computing the mass of several vehicles in literature. The outcomes are reported in Table 4 and they are deemed acceptable for the aim of the research, indeed, the percentage error is within ± 20 % for the considered cases. The reference values can be found in [10–13].

B. Aerodynamic Database Tool

During the atmospheric entry, the flight performance of the space vehicle is mainly driven by its aerodynamic behavior. The aerodynamic performance, in fact, plays a crucial role for the determination of its mission capabilities. Re-entry vehicles characterized by different aeroshapes and geometrical parameters will behave in distinct ways; the external shape, indeed, is one of the main factors in determining a vehicle's aerodynamic characteristic. In the context of missionisation, the shape of the vehicle can be conceived as an optimization variable, which must change within a wide range of layout during the process. Due to this fact, a complete aerodynamic characterization of the concept by exploiting Computational Fluid Dynamics (CFD) is not computationally feasible. In the same way, the use of simpler and less accurate methods, such as semi-empirical approaches, can be challenging, because they depends on a huge number of set-up parameters and the computational effort is still a bottleneck, especially if an MDA-MDO application is taken into account [14].

For these reasons, a dedicated aerodynamic tool has been developed, able to build a representative aerodynamic database for a wide range of re-entry vehicles. The tool is constituted by an AEDB based on interpolating functions obtained from datasets of aerodynamic coefficients computed by varying a prescribed number of geometrical parameters. The number of interpolating functions is given by subdiving the re-entry vehicles in categories. In this research, four

Table 3 Qualitative Inputs and Outputs parameters for the Geometry and Mass estimation tool.

	Parameter	Description
Inputs	$L, Diam, b, c$	Geometric parameters
	q_{dyn}, n_{load}	Sizing constraints
	Aerodynamic Density	Define the class of the re-entry vehicle
Outputs	S_{ref}	Reference surface of the vehicle
	m	Estimated mass of the vehicle

Table 4 Assessment of mass estimation by using the tool.

Name	Category	Mass tool (kg)	Mass Reference (kg)	Error %
Space Shuttle	WRV	68667	78000	-11.97
Horus 2B	WRV	26119	26029	0.35
Hopper	WRV	52556	60200	-12.70
X34	WRV	9812	8200	19.66
Hermes	WRV	14410	15000	-3.93
X38	WLB	10970	10659	2.93
HL-20	WLB	12565	10884	15.45
IXV	LB	1999	1900	5.14
Space Rider	LB	2710	2900	-6.53

classes are considered, defined by geometrical similarities and longitudinal aerodynamic performance (L/D). This last features, indeed, may be related to a variable called aerodynamic density (AD), which links the volume and the mass of the vehicle. Generally, the L/D increases by decreasing the aerodynamic density. Less dense vehicles, indeed, embed empennages and aerodynamic surfaces that decrease the density, but augment the L/D [3]. The datasets have been obtained by exploiting two tools provided by the German Aerospace Center (DLR) [14]. The categories included in this work are summarized in Fig. 4 and Table 5. For each category of re-entry vehicle, a dataset has been created by varying the flight conditions (angle-of-attack, Mach number), flight configuration (aerodynamic surface deflection) and geometrical parameters, then the AEDB is computed by interpolating the dataset onto the five dimensions. In this research, the geometrical parameters are the fineness ratio (L_{ref}/Diam) and the wing aspect ratio (ratio among wing span and mean aerodynamic chord). The obtained functions can be evaluated in any point of a particular domain with no additional computational burden, making this approach suitable for an MDA-MDO implementation. Figure 5 gives an overview of the developed aerodynamic Tool.

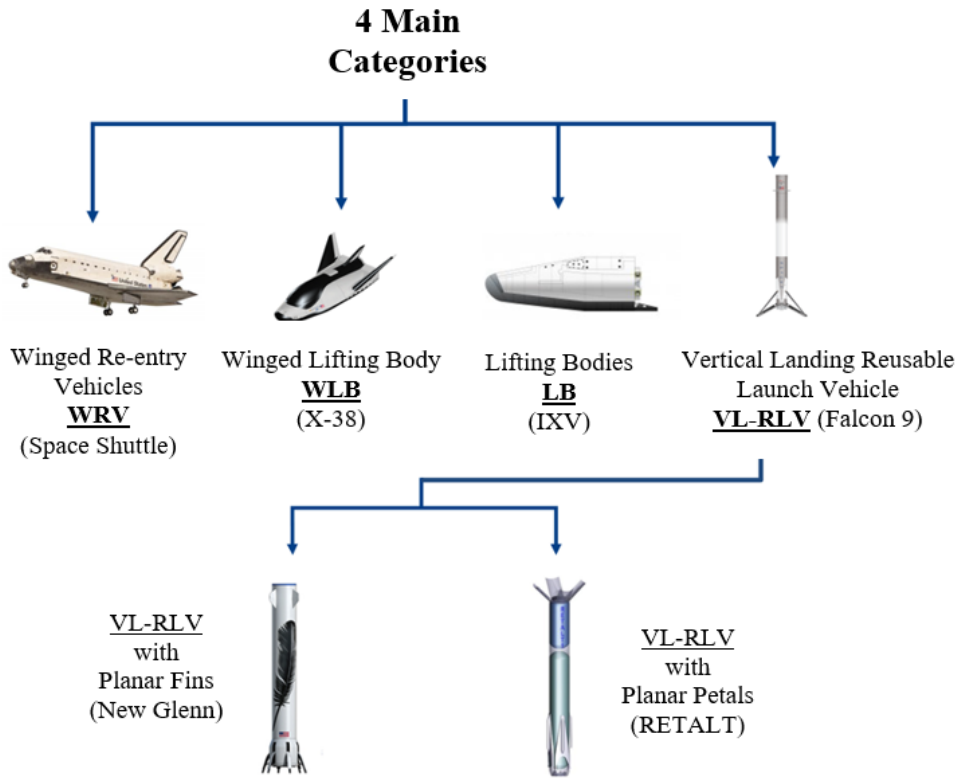

Fig. 4 Category subdivision of the re-entry vehicles [14]

Table 5 Re-entry vehicles classification.

Category	**AD** (kg/m^3)	**L/D** @ α 30º and Ma 5	**Example**
WRV	< 150	1.5	Space Shuttle
WLB	150 < AD < 250	1.2	X-38
LB	> 250	0.9	Space Rider
VL-RLV	-	-	Falcon9

The discipline included in the MDA stores the AEDB created with the procedure explained above and evaluates the interpolating functions with the geometrical parameters requested by the user. This method flaws in accuracy due to the assumptions made, but the outcomes are deemed acceptable for the purpose of the research. The user, however, is free to by-pass this disciplines and an accurate AEDB can be provided, if the shape of the vehicle is fixed and the AEDB is available. In Fig. 6, the capabilities of the tool are preliminary validated, by showing the estimation of the aerodynamic coefficients of Horus-2B with respect to the data available in literature [7]. Horus-2B is featured by a fineness ratio of 5, and a b/c of 1.7. The tool is able to estimate a representative AEDB of the vehicle considered. The trends are, in fact, reproduced with acceptable accuracy, especially in the hypersonic regime (Ma > 5). It can be noted, that the discrepancies increase at large Angle-of-Attack due to the rising of nonlinear effects. Table 6 summarizes the inputs and outputs of this disciplines. For further information, the reader is referred to [14].

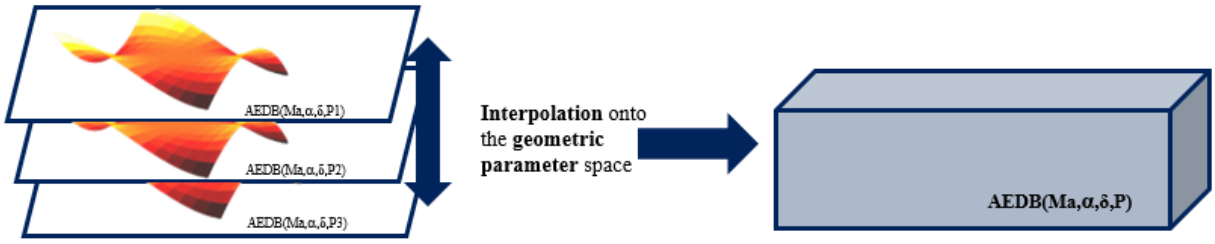

Fig. 5 High-Level idea for the building of the AEDB for one category [14]. P_i **are the geometrical parameters.**

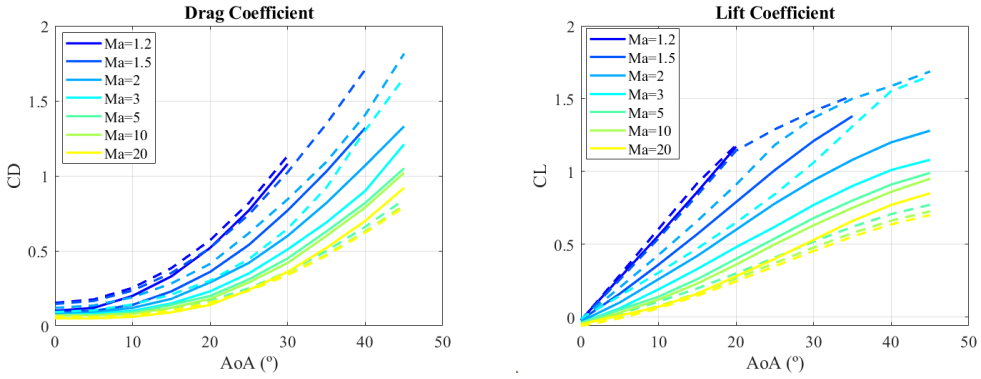

(a) Drag Coefficient vs AoA for different Ma

(b) Lift Coefficient vs AoA for different Ma

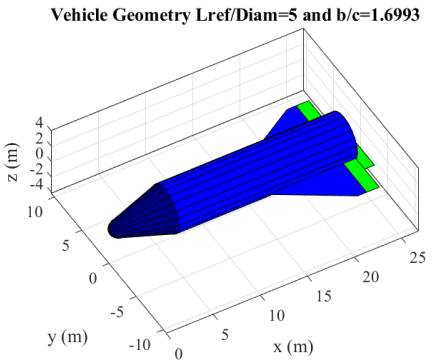

(c) Simplified geometry of Horus.

Fig. 6 Aerodynamic coefficients comparison and simplified geometry of Horus-2B. The dotted lines are the coefficients computed by the tool, while full lines are the literature data [7].

Table 6 Qualitative Inputs and Outputs parameters for the Aerodynamic Database Tool.

	Parameter	Description
Inputs	AoA, Mach range	Flight condition range
	Aerodynamic surface deflection range	Maximum and minimum deflection capability
	Fineness ratio, wing aspect ratio	Geometrical parameters to define the vehicle dimension
	Aerodynamic Density	Define the class of the re-entry vehicle
Outputs	C_D, C_L, and C_m	Aerodynamic Coefficients functions

C. Flying Quality Analyses Tool

A crucial step for the design of a re-entry mission include the Flying Quality Analysis (FQA). Summarizing, FQA computes the trim and stability capabilities of the vehicle. The outputs of this discipline are the so-called Angle-of-attack corridor, which is the domain in the α-Ma plane where the vehicle can fly in trimmed and stable configuration, the AEDB in the trimmed and stable configuration, and the Angle-of-Attack trim line defined within the corridor. The tool can also provide the information of the static margin. For the implementation of the tool, the following assumptions have been done:

- The tool is limited to the longitudinal trim and stability analysis;
- The aerodynamic of the control surfaces is described by an equivalent aerodynamic surface;
- The aerodynamic surface deflection is limited by user's define bounds;
- The tool deals with unpowered phases of the mission;

Briefly, the tool computes the trim deflection of the aerodynamic surface, if exists, and then evaluates the static longitudinal stability of that point, in the specified α-Ma domain, taking as input the untrimmed AEDB of the vehicle.

Generally, the AEDB of a vehicle is given by a function of the Mach number, Angle-of-Attack and the control surface:

$$\begin{aligned} C_D(Ma,\alpha,\delta) &= C_{D,clean}(Ma,\alpha) + \Delta C_D(Ma,\alpha,\delta) \\ C_L(Ma,\alpha,\delta) &= C_{L,clean}(Ma,\alpha) + \Delta C_L(Ma,\alpha,\delta) \\ C_m(Ma,\alpha,\delta) &= C_{m,clean}(Ma,\alpha) + \Delta C_m(Ma,\alpha,\delta) \end{aligned} \tag{2}$$

The trim conditions is given when the torques acting on the vehicles are zero, so when:

$$\exists \quad \hat{Ma},\hat{\alpha},\hat{\delta} \quad \text{such that} \quad C_m(\hat{Ma},\hat{\alpha},\hat{\delta}) = 0; \tag{3}$$

In this framework, only the longitudinal equilibrium is studied, so the analysis is done by considering the pitching moment coefficient. When Eq. (3) cannot be found in a certain flight conditions, the vehicle is said to be untrimmable. After having assessed the equilibrium points, the static longitudinal stability of the these points is evaluated with ESA-validated equations [15]. They compute the neutral point in order to obtain the static margin. If the static margin is greater than 0 in a specific point, then the vehicle is longitudinally stable. The evaluation of the static margin is performed by exploiting the aerodynamic coefficients expressed in body-frame: firstly, the axial and normal coefficients (C_A and C_N) must be defined:

$$\begin{aligned} C_A(Ma,\alpha,\delta) &= C_D\cos\alpha - C_L\sin\alpha \\ C_N(Ma,\alpha,\delta) &= C_D\sin\alpha + C_L\cos\alpha \end{aligned} \tag{4}$$

then, the static margin is computed by means of the following equations:

$$\begin{aligned} x_{np} &= \frac{C_m C_{A,\alpha} - C_{m,\alpha} C_A}{C_N C_{A,\alpha} - C_{N,\alpha} C_A} \\ sm_{sign} &= sign\left(\frac{C_N C_{A,\alpha} - C_{N,\alpha} C_A}{C_A}\right) \\ sm &= -sm_{sign}(x_{cog} - x_{np}) \end{aligned} \tag{5}$$

where $C_{(\cdot),\alpha}$ is the derivative of the coefficients with respect to the angle-of-attack. With the knowledge of the stability domain, it is possible to characterize the Angle-of-Attack corridor, i. e. the domain within which the trim line,

or Angle-of-Attack line, can be defined. This operation is performed automatically, by he FQA tool. The selection is ruled by a logic that sets the Angle-of-Attack close to maximum C_L condition. This selection allows to have a wider entry corridor at high Mach number. A different logic may be considered for future developments. If the MDA is embedded in an MDO framework, the trim line can be considered as a design variable, and its selection can be performed directly during the optimization process. As it is shown in the Section IV.D, the trim line is crucial for the design of the entry corridor, and thus the achievement of a safe re-entry trajectory for the aerothermal-mechanical view point.

Table 7 gives an overview of the inputs and outputs variables of the FQA tool. Figure 7 shows an example of the analyses performed with the FQA tool. The results have been obtained by considering the parameters in Table 8. Figure 7a shows the flap deflection needed to get the equilibrium, while Fig. 7b reports the static margin in the trim domain. The resulting stability domain is highlighted with the red lines. Figure 7c illustrates the Angle-of-Attack corridor and the selected trim line. In this case, the vehicle can fly in trim and stable configuration for the whole Ma-α domain taken into account.

D. Entry Corridor Analysis

During the design of a re-entry mission a fundamental analysis is the definition of the so-called entry corridor. The entry corridor is the domain where the vehicle can fly without violating the aerothermal-mechanical loads bounds. This analysis is crucial for designing safe re-entry trajectories.

The entry corridor is typically given in the drag-energy space, by exploiting the energy as independent variable, or in the altitude-velocity space, by using the velocity as independent variable. For the implementation of this discipline, the following assumptions have been considered [16, 17]:

- The tool computes the domain for the aerodynamic phase of the flight. In this phase, the vehicle is unpowered;
- The energy is the independent variable (as said previously, the velocity can be used alternatively);
- The tool asks as inputs the AEDB of the vehicle and the angle-of-attack profile. The angle-of-attack can be also provided as a fixed parameter to perform parametric analysis;
- The considered aerothermal-mechanical constraints are:
  - Maximum dynamic pressure;
  - Maximum heat flux at stagnation point (Chapman's Equation [16]);
  - Maximum g-load;

Table 7 Qualitative Inputs and Outputs parameters for the FQA tool.

	Parameter	Description
Inputs	AoA, Mach range	Flight condition range
	Control surface deflection range	Maximum and minimum deflection capability
	CoG shift	Delta CoG position for the computation of the trim
	AEDB	Aerodynamic Database of the vehicle
Outputs	AoA corridor	Trimmability and stability region
	AoA trim line	Angle-of-Attack line for the definition of the trajectory
	Trim deflection	Deflection of the aerodynamic surface to trim the vehicle
	SM	Values of the static margin
	Trimmed AEDB	AEDB in trimmed configuration

Table 8 Parameters for the analysis showed in Fig. 7.

Parameter	Value	Unit	Parameter	Value	Unit
AoA range	[0, 45]	º	L_{ref}	25	m
Ma range	[2, 25]	-	X_{cog}	0	m
N_α	51	-	Z_{cog}	0	m
N_{Ma}	51	-	ΔX_{cog}	0	m
δ_{min}	-20	º	ΔZ_{cog}	0	m
δ_{max}	30	º			

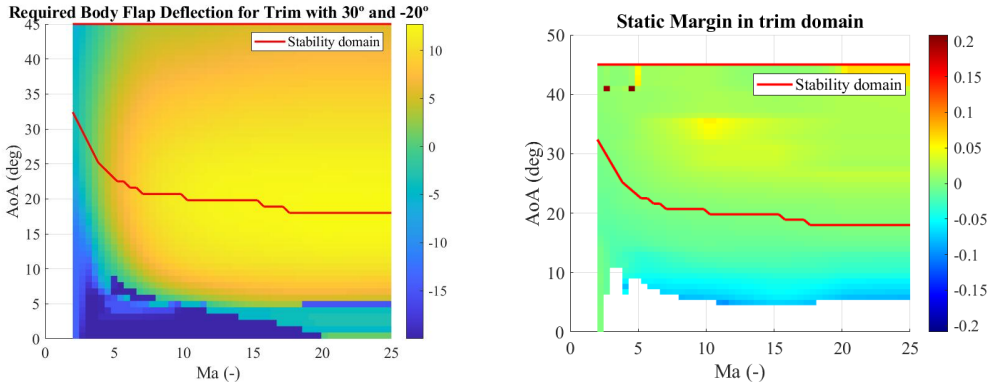

(a) Required deflection for trim.

(b) Static Margin evaluation.

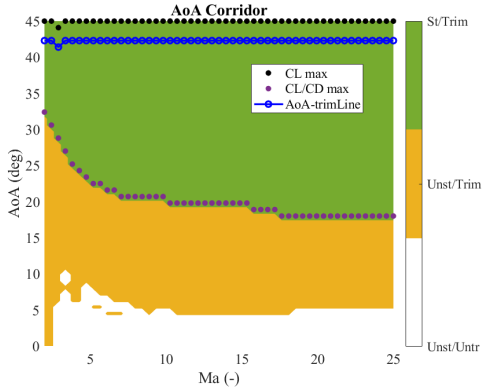

(c) Angle-of-Attack Corridor and trim line.

Fig. 7 FQA outputs for Horus-2B.

– Equilibrium glide (or terminal velocity for vehicle with low L/D);

When the energy is used as independent variable, the bounds of the entry corridor can be computed by solving a set of systems of nonlinear equations. The energy and the aerothermal-mechanical constraints equations, in fact, depend on the velocity and altitude. Therefore, for each of the constraints, and each energy level, it is possible to solve the system of nonlinear equations, obtaining the altitude and velocity couple which generates the maximum value of the specific constraint. The first equation of the set of systems is given by the equation of the specific energy:

$$\frac{V^2}{2} - \frac{\mu}{h + r_p} = \bar{E} \tag{6}$$

Where $\bar{E}$ is the prescribed energy value. The second equation, instead, describes the considered aerothermal-mechanical constraint. In this paper, these equations are:

$$\frac{1}{2}\rho(h)V^2 = \bar{q}_{dyn,max} \tag{7}$$

$$\frac{C_0}{\sqrt{R_{nose}}}\sqrt{\rho(h)}V^{3.15} = \dot{\bar{q}}_{heat,max} \tag{8}$$

$$(g(h) - \frac{V^2}{h + r_p}) - L = 0 \tag{9}$$

For vehicles characterized by low lift. the terminal velocity is considered, and the Eq.(9) is substituted by $W = D$. One of the drawbacks of the equilibrium glide condition presented above is given by the assumptions done. Equation (9)

does not take into account the terms relative to the planet rotation, and the Flight-Path-Angle (FPA) and the bank angle are considered equal to zero. An alternative approach for the definition of the equilibrium glide drag profile consists of the development of a Flight-Path-Angle tracking control. The feedback controller schedules the bank angle to track a reference FPA, which it can be considered relatively small to increase the range capabilities. This approach accounts for the Planet rotation and reduces the phugoid motion. The feedback controller can be done using a first-order dynamics [18], given by:

$$(\gamma'_{ref} - \gamma') + K_\gamma(\gamma_{ref} - \gamma_{ref}) = 0 \tag{10}$$

and replacing it in the dynamic equations of motion of the FPA written in function of the specific energy, it is possible to have:

$$\frac{L}{D}\cos\sigma = \left(g - \frac{V^2}{r}\right)\frac{\cos\gamma}{D} + V^2(C_\gamma - K_\gamma(\gamma_{ref} - \gamma) - \gamma'_{ref}) \tag{11}$$

where C_γ includes the terms due to the Planet rotation, while K_γ is a constant for the feedback control [18]. By propagating the equations of motion with Eq. 11, it is possible to get the trajectory and the associated drag profile.

By solving the four systems of equations given by Eq.(6), and Eqs. (7), (8, (9), the altitude and velocity profiles that make active the constraints are obtained. From these profiles, the corresponding drag accelerations are given:

$$D_{qdyn,max} = \frac{1}{2}\rho(h_{qdyn})V_{qdyn}^2\frac{S_{ref}}{m}C_D(Ma(h_{qdyn}, V_{qdyn}), \alpha) \tag{12}$$

$$D_{qheat,max} = \frac{1}{2}\rho(h_{qheat})V_{qheat}^2\frac{S_{ref}}{m}C_D(Ma(h_{qheat}, V_{qheat}), \alpha) \tag{13}$$

$$D_{g,max} = \frac{1}{2}\rho(h_g)V_g^2\frac{S_{ref}}{m}C_D(Ma(h_g, V_g), \alpha) \tag{14}$$

$$D_{eg} = \frac{1}{2}\rho(h_{eg})V_{eg}^2\frac{S_{ref}}{m}C_D(Ma(h_{eg}, V_{eg}), \alpha) \tag{15}$$

where $h_{(.)}$ and $V_{(.)}$ are the altitude and velocity profiles relative to the considered constraint. The entry corridor in drag-energy space is defined by the equilibrium glide drag profile for what concerns the lower bound, and by the minimum value for each energy level among the aerothermal-mechanical constraints:

$$u_b = \min(D_{qdyn,max}, D_{qheat,max}, D_{g,max}) \tag{16}$$

It is worth to mention that the shape of the entry corridor is affected by the selection of the angle-of-attack profile, meaning that this discipline is directly linked to the output of the FQA tool. Table 9 summarizes the inputs and outputs parameters associated to this disciplines.

Figure 8 shows the entry corridor obtained for Horus-2B with the values reported in Table 2. For this analysis, it has been considered an initial velocity of 7.5 km/s at 100 km of altitude, till the TAEM interface with final velocity of 0.6 km/s and final altitude of 30 km. The atmosphere has been modeled with the US76 model [19].

Table 9 Qualitative Inputs and Outputs parameters for the Entry Corridor tool.

	Parameter	**Description**
Inputs	AoA profile	Angle-of-attack trim line
	AEDB	Aerodynamic Database of the vehicle
	Vehicle dimensions	Reference dimension of the vehicle (such as S_{ref})
	Vehicle mass	Mass of the vehicle
	Loads values	Maximum values of the aerothemal-mechanical constraints
	Environment	Environmental properties of the planet
Outputs	Entry Corridor bounds	Upper and lower feasible drag profiles
	AoA trim line	Updated trim line if the corridor is closed

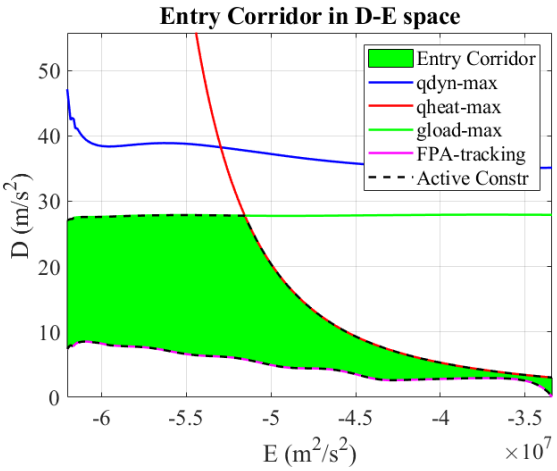

Fig. 8 Entry Corridor for Horus-2B.

The entry corridor tool is also able to evaluate the entry corridor with respect the ballistic coefficient (BC) and the FPA at Entry-Interface-Point (EIP). This analysis, which is relevant for ballistic and uncontrolled trajectories and when the design of the vehicle is not fixed, identifies the envelope, defined in terms of BC and FPA at EIP, that fulfils all imposed constraints. Moreover, it determines eventual skipping trajectories.

1. Initial Flight-Path-Angle computation

A secondary functionality of the Entry Corridor tool is the automatic computation of the initial FPA if the user does not set up it in the input file. For specific entry conditions (velocity and altitude), the tool evaluates the minimum FPA to avoid skipping trajectories (grey zone in Fig. 9), and the maximum FPA to avoid trajectories that would violate the aerothermal-mechanical constraints. The tool will use this information for the computation of the equilibrium glide profile, and for the estimation of the range capabilities. Figure 9 shows an example of this kind of analysis for Horus-2B with an EIP velocity of 7.5 km/s. The figure shows the feasible range of FPA for the specified velocity, but it gives an insight into the initial FPA and velocity sensitivity for the entry corridor performance. The yellow band has the scope to highlight the feasible region. This analysis may be used also before running the full MDA to help the user to set up correctly a feasible initial FPA.

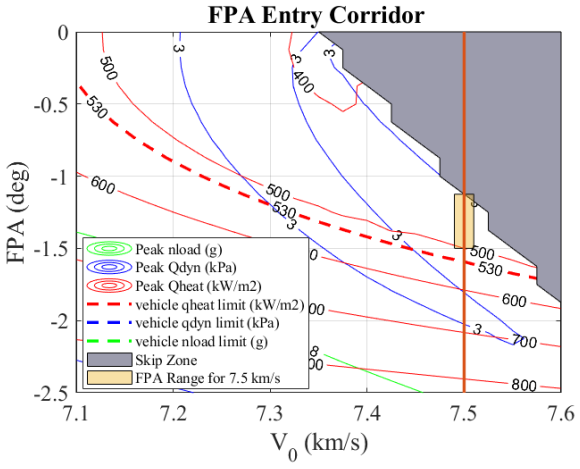

Fig. 9 Example of Entry Corridor for Horus-2B with respect to the initial FPA.

E. Range Capabilities

A critical capability for the mission analysis of an entry vehicle is to estimate, from any EIP conditions, the landing footprint, thus the set of reachable landing sites. A landing site is feasible if the vehicle can reach it without violating any safety constraints regarding the vehicle or the crew. To calculate the reachable area, the boundary points of the landing footprint should be determined. A possible approach is to solve a set of optimal control problems, but the high computational effort is an issue, especially for an MDA-MDO implementation. In the frame of this research, it has been followed the approach presented in [18], which is based on the Evolved Acceleration Guidance Logic for Entry (EAGLE) [20]. The EAGLE planner designs feasible trajectories, considering the vehicle constraints and Coriolis effects. This method computes the range capabilities of the vehicle by exploiting the information computed with the Entry Corridor tool. Each trajectory is generated based on a drag profile which is defined within the entry corridor bounds. From the drag profile, it is possible to obtain a bank control used to get the trajectory. A step forward with respect to the state-of-the-art was to generalize the algorithm for what concerns the considered atmospheric model. In this research, any kind of atmospheric model can be used, while in [18] an exponential model was assumed.

In order to estimate the footprint, the algorithm exploits a set of drag profiles that span the entry corridor. The drag profiles are computed by interpolating the lower bound drag profile, which gives the far-edge endpoint of the footprint, and the upper bound drag profile, which provides the near-edge endpoint of the footprint. The interpolation is defined by:

$$D(E) = D_{max}(E) + a(D_{min}(E) - D_{max}(E)) \tag{17}$$

with $a \in [0,1]$. Figure 10b shows the feasible drag profiles used to obtain the footprint. The minimum and maximum drag profiles have been modified to match the boundary conditions. Moreover, the maximum drag profile has been smoothed in the proximity of those points in which the active constraint changes. After having computed the drag profiles, the trajectories are created by scheduling the bank through the following equations:

$$\frac{L}{D}\cos\sigma = \frac{1}{b}(D'' - a) \tag{18}$$

where

$$\begin{aligned} a &= D\left(\frac{C_D''}{C_D} - \frac{C_D'^2}{C_D^2}\right) + D'\left(\frac{C_D'}{C_D} + \frac{2}{V^2}\right) - \frac{4D}{V^4} + \frac{1}{DV^2}\left(\frac{\rho_h}{\rho} - 2\frac{g}{V^2}\right)\left(\frac{V^2}{r_p + h} - g\right) + \left(\frac{2g}{V^2} - \frac{\rho_h}{\rho}\right)C_\gamma \\ b &= \frac{1}{V^2}\left(\frac{\rho_h}{\rho} - 2g/V^2\right) \end{aligned} \tag{19}$$

where C_γ is the term related to the rotation of the planet [18], while ρ_h is the derivative of the density with respect to the altitude. Thus, the bank angle is:

$$|\sigma| = \cos^{-1}\left(\frac{D}{bL}(D'' - a)\right) \tag{20}$$

Equation (20) gives only the magnitude of the bank angle, so the right and the left-edge are computed by considering the bank always positive and negative during the flight (Fig. 10c). To define the farthest and the nearest edges, reversal bank maneuvers may be considered. A simplification is to assume them as straight lines. In the case in which the user specifies a target point, the tool can evaluate the minimum distance between the footprint bound and the prescribed uncertainty ellipse of the target point.

In conclusion, Table 10 summarized the I/O related to this discipline, while Fig. 10a shows the resulting footprint for Horus-2B with the initial altitude and velocity specified in Table 2, 0º latitude, 0º longitude and 45º heading angle.

F. Trajectory Optimization Tool

In the context of mission analysis and design, a trajectory optimization routine is a crucial analysis that must be performed. Trajectory optimization is the technique of designing a trajectory that minimizes or maximizes a prescribed performance quantity while satisfying a set of constraints. It is a subcase of a more general optimal control problem [21, 22]. The generation of an entry trajectory is, indeed, a constrained optimization problem. These constraints include particular path constraints, some limitations on the control action that can be applied, and boundary conditions. In general, the entry and landing problem is a multi-phase optimization problem and each phase can be characterized by different constraints and objectives. This discipline is mandatory for what it concerns with the first objective of the

Table 10 Qualitative Inputs and Outputs parameters for the Range Capabilities Tool.

	Parameter	Description
Inputs	AoA profile	Angle-of-attack profile
	AEDB	Aerodynamic Database of the vehicle
	Vehicle dimensions	Reference dimension of the vehicle
	Vehicle mass	Mass of the vehicle
	Entry Corridor bounds	Upper and lower fesible drag profiles
	Boundary Conditions	Entry (at EIP) and final conditions
	Target point	Target point coordinates
	Uncertainty ellipse	Uncertainty ellipse about the target point
Outputs	Range capabilities	Feasible footprint domain
	Bank profiles	Scheduled bank profiles
	Min distance	Minimum distance between footprint bounds and the ellipse

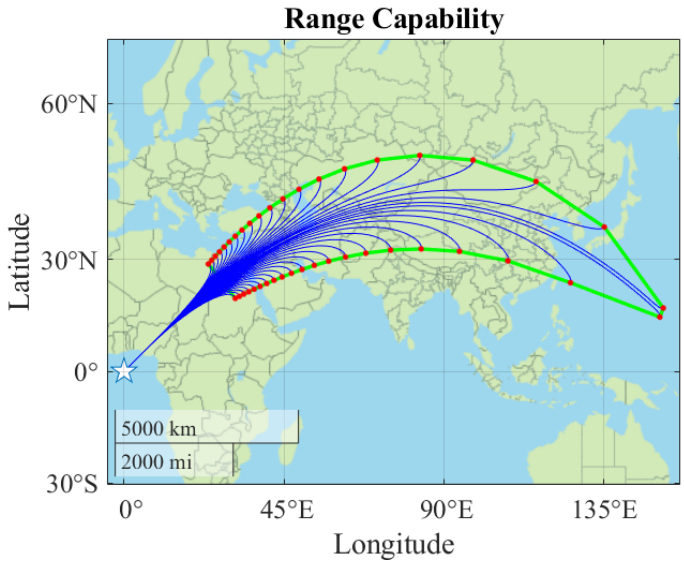

(a) Estimated range capabilities. The trajectories are in blue, the red dots are the end-points, the green lines mark the footprint, while the white star denotes the EIP.

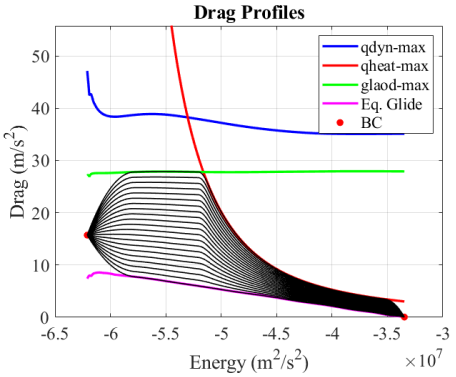

(b) Interpolated drag profiles.

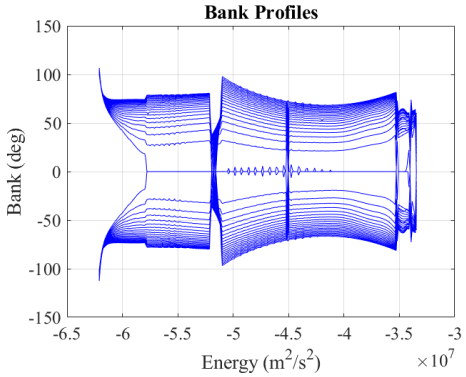

(c) Bank profiles associated to the drag profiles.

Fig. 10 Range Capabilities analysis for Horus-2B, with initial condition reported in Table 2, 0º latitude, 0º longitude and 45º heading angle.

missionisation tool, which is the adaptation of the mission analysis and GNC to a particular mission. Depending on the particular requirements and features of a specific mission, the tool can adapt the solution by computing the optimum trajectory and mission profile. For this reason, a multi-phase trajectory optimization discipline has been embedded in the missionisation tool. The trajectory optimization tool may be used both after the MDO for the design of the final trajectory once the performance maps and the mission capabilities of the vehicle have been assessed, and within the MDO routine for the optimal tuning of the design parameters of the other disciplines. In this second application, the computational effort will be high due to the nested optimization routine.

Within this research, the optimal control problem is solved by transforming it into a Nonlinear Programming Problem (NLP) with Hermite-Simspon direct transcription method. The unknowns are the state and control variables, as well as n-parameters such as the final time of each phase. Then the NLP is solved by using a Sequential Quadratic Programming (SQP) algorithm [23] available in MATLAB toolbox. A dedicated tool has been developed for the numerical computation of the gradients of the constraints and the objective to improve and speed up the convergence. Moreover, a general input file has been created that allows the user to describe the considered problem. The reasons for this choice are driven by the fact that a direct collocation method is more robust with respect to a shooting methods concerning the selection of the initial guess. Moreover, it is faster than heuristic method such as the genetic algorithm. However, it must be taken in mind that a gradient-based algorithm depends on the initial guess and the convergence to the global optimum is not guaranteed [21, 22].

The tool has been tested and validated among several examples, including the brachistochrone problem [24]. Below the maximum crossrange problem is reported. The objective is the maximization of the crossrange for a prescribed downrange for a lifting re-entry vehicle. The results are compared with those of the Footprint Evaluation tool for validation purposes.

1. Maximum crossrange problem

In this example, the maximum crossrange problem is solved [25]. It is defined to maximize crossrange when downrange is specified. This problem is an interesting example due to the nonlinear dynamics, terminal constraints, and path constraints. Moreover, this example has been used to compare and validate the outcomes obtained by the Footprint Evaluation Tool.

The problem has been modeled with 3DoF equations of motion in the spherical rotating reference frame. The control variable is the bank rate. So the problem is ruled by the following equations of motion [16]:

$$
\begin{aligned}
\dot{h} &= V\sin(\gamma)\\
\dot{\theta} &= \frac{V\cos(\gamma)\sin(\psi)}{R\cos(phi)}\\
\dot{\phi} &= \frac{V\cos(\gamma)\cos(\psi)}{R}\\
\dot{V} &= -D - g\sin(\gamma) + \omega_E^2 R\cos(\phi)(\sin(\gamma)\cos(\phi) - \cos(\gamma)sin(\phi)\cos(\psi))\\
\dot{\gamma} &= \frac{L\cos(\sigma)}{V} + \left(\frac{V}{R} - \frac{g}{V}\right)\cos(\gamma) + 2\omega_E\cos(\phi)\sin(\psi) +\\
&\quad + \frac{\omega_E^2 R}{V}\cos(\phi)(\cos(\gamma)\cos(\phi) + \sin(\gamma)\sin(\phi)\cos(\psi))\\
\dot{\psi} &= \frac{L\sin(\sigma)}{V\cos(\gamma)} + \frac{V}{R}\cos(\gamma)\sin(\psi)\tan(\phi) - 2\omega_E(\tan(\gamma)\cos(\phi)\cos(\psi) - \sin(\phi)) +\\
&\quad + \frac{\omega_E^2 R}{V\cos(\gamma)}\sin(\phi)\cos(\phi)\sin(\psi)\\
\dot{\sigma} &= u
\end{aligned}
\tag{21}
$$

where u is the control variable. In this report, it is assumed that the Angle-of-Attack profile is given, so the bank rate is the only control. The atmosphere has been modeled with US76 model. The Earth is considered spherical with a mean radius of 6371 km, so that the gravity is defined as $g(r) = \frac{\mu}{(r_p+h)^2}$, with μ equal to 3.986×10^{14} m^3/s^2. ω_E is the angular velocity of the Earth and it is equal to 7.2921159×10^{-5} rad/s.

Path constraints are the maximum allowed heating rate, the dynamic pressure, the normal load, and the quasi-equilibrium glide [20] condition are given by:

$$
\begin{aligned}
&\dot{q}_{heat} = C_1 \frac{\sqrt{\rho}}{\sqrt{R_n}} V^{3.15} \leq \dot{q}_{heat,max} \\
&q_{dyn} = 0.5\rho V^2 \leq q_{dyn,max} \\
&n_{load} = \sqrt{L^2 + D^2} \leq n_{load,max} \\
&D(h, V, \alpha) \geq D_{qs,min}
\end{aligned}
\tag{22}
$$

Where C_0 is a constant, and ρ is the atmospheric density. Moreover, the bank rate is bounded with:

$$
-\dot{\Sigma} \leq \dot{\sigma} \leq \dot{\Sigma} \tag{23}
$$

where $\dot{\Sigma}$ is a constant with dimension rad/s. Moreover the initial and final conditions are enforced:

$$
\begin{aligned}
&\boldsymbol{x}_0 = [h_0 \quad \theta_0 \quad \phi_0 \quad V_0 \quad \gamma_0 \quad \psi_0] \\
&\boldsymbol{x}_f = [h_f \quad \theta_f \quad V_f]
\end{aligned}
\tag{24}
$$

Without loss of generality, this paper shows the case in which the entry vehicle at the entry point is flying along the Equator. In this special case, the maximization of the crossrange corresponds with the maximization of the final latitude, while the downrange is given by the longitude. For this reason, the cost function is:

$$
J = -\phi_f \tag{25}
$$

For the general case, the reader can find more information in [25]. So, the maximum crossrange problem can be summarized by:

$$
\begin{aligned}
&\text{minimise} \quad J = -\phi_f \\
&\text{subject to} \\
&\quad \dot{\boldsymbol{x}} = \boldsymbol{f}(\boldsymbol{x}, u) \qquad \text{Eq. (21)} \\
&\quad C_0 \frac{\sqrt{\rho}}{\sqrt{R_n}} V^{3.15} \leq \dot{q}_{heat,max} \\
&\quad 0.5\rho V^2 \leq q_{dyn,max} \\
&\quad \sqrt{L^2 + D^2} \leq n_{load,max} \\
&\quad D(h, V, \alpha) \geq D_{qs,min} \\
&\quad -C \leq \dot{\sigma} \leq C \\
&\quad \boldsymbol{x}_0 = [h_0 \quad \theta_0 \quad \phi_0 \quad V_0 \quad \gamma_0 \quad \psi_0] \\
&\quad \boldsymbol{x}_f = [h_f \quad \theta_f \quad V_f]
\end{aligned}
\tag{26}
$$

For this example, the considered vehicle is Horus-2B, featured by the parameters in Table 2, while the boundary conditions and constraints on the control are available in Table 11. It is worth to mention, that due to complexity of the problem, a constraints-relaxed problem with a rough initial guess has been solved first. Then, the solution has been used as initial guess for the complete problem.

Figure 11 shows the results of the maximum crossrange problem. The solver gives a maximum crossrange of about 8.79º, which corresponds to 977.46 km. The constraints are respected, as reported in Fig. 11f and Fig. 11i. By considering these two figures, it can be noted that the heat flux constraints is active for this case, and the results of the entry corridor analysis are coherent with the ones computed by the optimization process.

In order to validate both these results and the Footprint Evaluation tool (Section IV.F), the maximum crossrange problem has been solved by varying the downrange, to obtain the footprint. The comparison is shown in Fig. 12. The obtained results are satisfactory, in fact, the footprints are very similar. The one computed with the optimization problem is larger, as may be expected. This outcome has been reported also by [25], underlying the goodness of the results. Also in this case, the near and the far edges have been assumed straight lines, without considering bank reversal maneuvers.

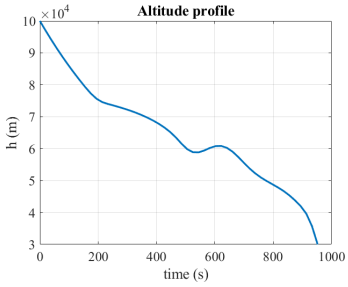

(a) Optimal altitude profile.

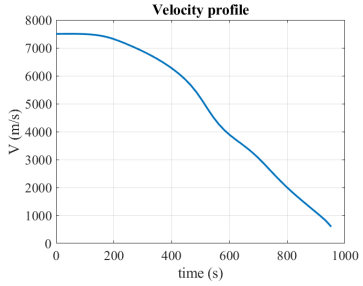

(b) Optimal Velocity profile.

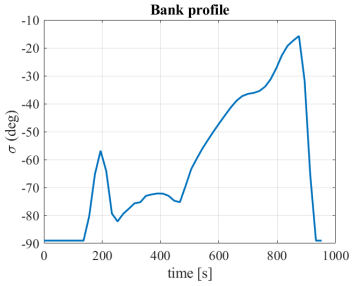

(c) Optimal bank profile.

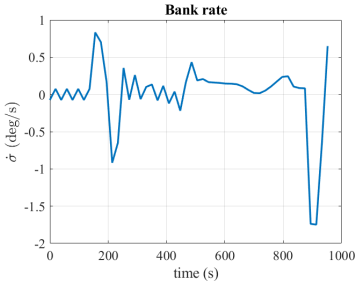

(d) Optimal bank rate profile.

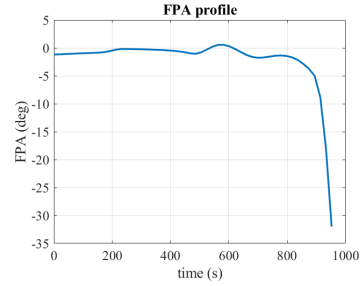

(e) Optimal FPA profile.

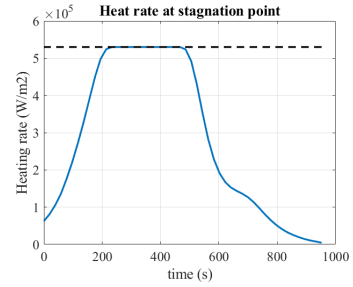

(f) Heat flux profile.

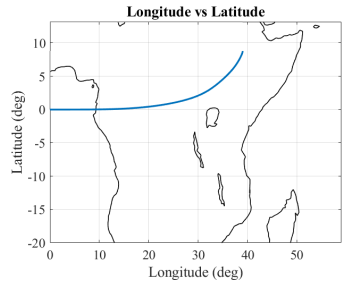

(g) Optimal trajectory in Longitude-Latitude plane.

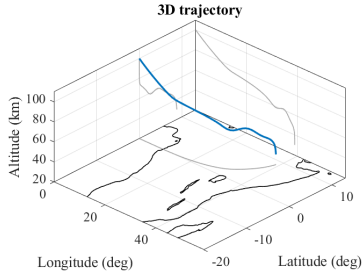

(h) 3D trajectory in Longitude-Latitude-Altitude axes.

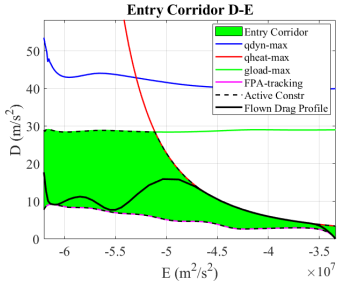

(i) Entry Corridor and optimal drag profile.

Fig. 11 Results of the maximimum crossrange problem.

Table 11 Boundary conditions and control bounds for the crossrange maximisation

Parameter	Value	Units	Parameter	Value	Units
Initial altitude	100	km	Final altitude	30	km
Initial velocity	7.5	km/s	Final velocity	0.6	km/s
Initial latitude	0	º	Final latitude	free	º
Initial longitude	0	º	Final longitude	39	º
Initial FPA	-1.2	º	Final FPA	free	º
Initial heading	90	º	Final heading	free	º
σ_0	free	º	σ_f	free	º
$\|\|\sigma_{min}\|\|$	1	º	$\|\|\sigma_{max}\|\|$	90	º
$\dot{\sigma}_{min}$	-5	º	$\dot{\sigma}_{max}$	5	º
t_0	0	s	t_f	free	s

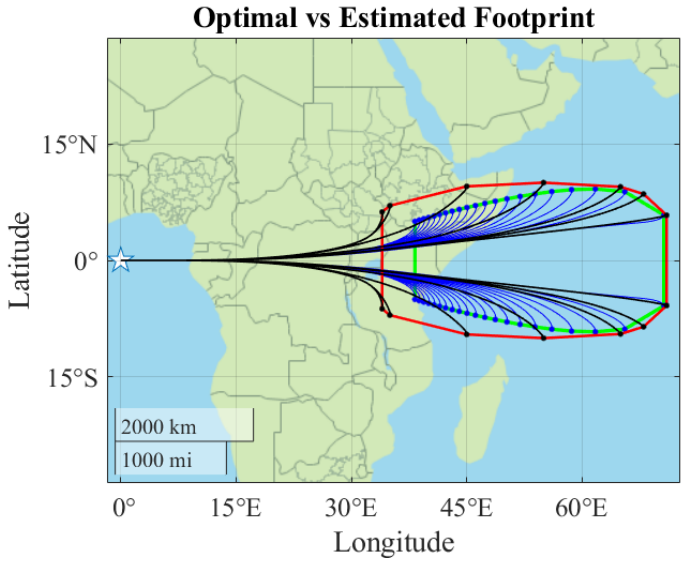

Fig. 12 Optimal (in red) and estimated footprint (in green).

V. MDO Methodologies Overview

As introduced in Section III, an MDO routine is foreseen for answering especially the second objective of the tool, and it will constitute the so-called Missionisation layer. The implementation of MDO faces two key problems in practical engineering. The first problem is given by the management of the coupling of multiple disciplines, and so the architecture of the MDO. The simplest approach is to develop an MDA environment through a single-level black-box optimization, in which the coupling variables are iteratively solved. In addition, several MDO architectures have been developed to organize the analysis model and the computational flow. Generally, the architectures are categorized as monolithic and distributed architectures [5, 26]. The first group includes At-All-Once (AAO), Individual Discipline Feasible (IDF), and Multidisciplinary Feasible (MDF); the second group comprises, for instance, Collaborative Optimization (CO). A clear hierarchy cannot be defined, the effectiveness and efficiency of each architecture are, indeed, directly related to the features of the problem being solved [27]. The second crucial problem concerns with the efficiency in solving MDO problems with limited computational resources, in fact the design involves high-fidelity models and iterative MDA processes which are expensive to evaluate. Moreover, lots of practical applications are nonconvex problem with a large number of local optima, which complicate the convergence to the global optimum of the problem.

Classical algorithms used to solve MDO problems can be divided into two main groups:

- **Gradient-based algorithms**: these algorithms exploit the information from the gradient of the constraints and cost function to compute a search direction toward feasibility and optimality. This group includes Sequential Quadratic Programming algorithms and open-source tools exist like openMDAO [6, 28].
- **Global Optimization Algorithms**: these algorithms are based on heuristic and metaheuristic methods to converge to the global optimum of the problem. Examples of these algorithms are Genetic Algorithm (GA) and Particle Swarm Optimization (PSO).

Both methodologies have advantages and drawbacks. For gradient-based algorithms, the convergence is affected by the selection of the initial starting guess and the optimizer may converge to a local optimum. However, if the gradient can be computed efficiently, the computational cost of these methods may be far less with respect to global optimization. A limitation is that these methods are not well suited for multi-objective optimization. To overcome this issue, several methods have been developed to obtain multi-objective solutions with local algorithms without exploiting the gradients, or by using optimality concepts from game theory [26]. For what concerns global optimization algorithms, the information of the gradient and the initial guess are not necessary, in fact, they rank the solution depending on the constraints violation and the objective function, and update the solution by exploiting a random search and imitating nature-based heuristic methods, starting from a randomly-defined initial guess. Moreover, these methods are suitable for handling multiple objectives [6, 26]. On the other side, global algorithms require a larger number of function evaluations, resulting in a slow convergence, and they are very sensitive to the setting parameters. For these reasons, global and local algorithms are used in synergy by exploring the domain first and then refining the solution.

A. Metamodeling Techniques

As introduced above, the computational effort depends on the definition of MDO architecture and the evaluation of the disciplines. To reduce the computational cost of expensive black-box optimization problems, metamodel-based design optimization (MBDO) techniques have been developed. In this case, the MDO problem is treated as a constrained nonlinear optimization problem, in which the MDA process is replaced by a surrogate model.

In literature, there are several Metamodel-based MDO methods, which can be classified as static and dynamic. In the first case, the metamodels are created once based on sufficient samples; in the second one the metamodels are adaptively refined during the optimization process. It is worth mentioning that the accuracy of the prediction of the metamodels must be verified in order to ensure the reliability of the outcomes. Some techniques used to create the metamodel are:

- **Polynomial response surface method**: this method exploits a multivariate linear regression function to fit the simulation model or the MDA process;
- **Radial basis functions**: this approach is an interpolation method based on the function value at the sample points;
- **Kriging** this technique uses optimal estimation interpolation model by combining a global approximation model and stochastic process;
- **Artificial Neural Networks**: this method employs artificial neural networks to approximate the nonlinear functions. This group includes Feed-Forward Neural Networks (FFNN) and Radial-Basis Function Neural Networks (RBFNN);
- **Multivariate Adaptive Regression Splines (MARS)**: it is a regression procedure that automatically models nonlinearities and interactions through fitting functions.
- **Support Vector Regression (SVR)**: this technique is one of the most popular supervised learning algorithms, which is used for classification and regression problems

These techniques have unique features and the most suitable one depends on the problem itself. Two criteria that may be taken into account for the selection of the metamodel method are the accuracy of the prediction [5], and the computational effort needed to build the surrogate model.

VI. Conclusion

The growing need to find more economic, ecological, and sustainable solutions for space access has led space agencies and private companies to invest in the development of reusable space vehicles both for space access and in-orbit studies. The capability of a space transportation system to be adapted to specific missions and to be able to perform multiple mission scenarios, especially for what concerns the Entry, Descent, and Landing phase, prompt the necessity of a Mission Analysis and GNC missionisation process and tool for autonomous re-entry vehicles which reduces the tailoring efforts between each re-flight and mission.

This paper gives an overview of the MA and GNC missionisation process and tool proposed in this research within ASCenSIon. Starting from the definition and the objectives of missionisation within this research, the High-Level architecture of the tool has been reported, by underlying which are the components of the tool and the reason why they have been selected. The first goal aims at adapting the MA and GNC solution for one specific mission, while the second targets the evaluation of the mission performance in order to find one solution capable of performing multiple missions. Due to the fact that missionisation is a multidisciplinary problem, the set of disciplines identified within the architecture must be correctly set up to build the MDA. A crucial step is the identification of the interactions between them in order to understand the I/O relations and the presence of loops. So the report gives an overview and an example of the DSM analysis. Then, the engineering modeling of the disciplines within the MDA framework is reported, underlying the assumptions, the design choice, and the mathematical models. Some examples of analyses are reported to show their performance, exploiting Horus-2B as a baseline vehicle. Particular attention has been given to the input parameters each discipline needs, as well as the outputs computed. Lastly, the report gives an overview of the MDO for the development of the missionisation layer. Metamodel-based MDO approaches seem to be a promising solution for reducing the computational effort requested to solve the MDO.

Future work foresees the integration of the MDA with the Missionisation Layer and the application of the tool to several real-case scenarios both for Preliminary Mission Design and Missionised Solution.

Acknowledgments

The project leading to this application has received funding from the European Union's Horizon 2020 research and innovation program under the Marie Skłodowska-Curie grant agreement No 860956.

References

[1] Bernard, M., "Vega Missionization and Post Flight Analyses," Ph.D. thesis, Sapienza Università di Roma, 2009.

[2] Harpold, J., and Graves Jr, C., "Shuttle entry guidance," *American Astronautical Society*, 1978.

[3] Medici, G., De Zaiacomo, G., Bonetti, D., Pina, F., and Yabar, C., "Multi-Disciplinary Optimisation of Re-entry Vehicles from TAEM to Landing," *7th European Conference for Aeronautics and Space Science (EUCASS)*, 2017. https://doi.org/10.13009/EUCASS2017-413.

[4] Lambe, A. B., and Martins, J. R., "Extensions to the design structure matrix for the description of multidisciplinary design, analysis, and optimization processes," *Structural and Multidisciplinary Optimization*, Vol. 46, No. 2, 2012, pp. 273–284.

[5] Shi, R., Long, T., Ye, N., Wu, Y., Wei, Z., and Liu, Z., "Metamodel-based multidisciplinary design optimization methods for aerospace system," *Astrodynamics*, Vol. 5, No. 3, 2021, pp. 185–215.

[6] Castellini, F., "Multidisciplinary Design Optimization for Expendable Launch Vehicles," Ph.D. thesis, Politecnico di Milano, 2012.

[7] Mooij, E., "The HORUS-2B Reference Vehicle," , 1995.

[8] Harloff, G., and Berkowitz, B., "HASA: Hypersonic Aerospace Sizing Analysis for the preliminary design of aerospace vehicles," 1988.

[9] Viviani, A., Iuspa, L., and Aprovitola, A., "An optimization-based procedure for self-generation of Re-entry Vehicles shape," *Aerospace Science and Technology*, Vol. 68, 2017, pp. 123–134.

[10] Weiland, C., *Aerodynamic data of space vehicles*, Springer Science & Business Media, 2014.

[11] Hirschel, E. H., and Weiland, C., *Selected aerothermodynamic design problems of hypersonic flight vehicles*, Vol. 229, Springer Science & Business Media, 2009.

[12] Jackson, E., Cruz, C., and Ragsdale, W., "Real-time simulation model of the HL-20 lifting body," Vol. 92, 1992.

[13] Haya Ramos, R., Bonetti, D., Serna, J., De Zaiacomo, G., and Caramagno, A., "Validation of the IXV Mission Analysis and Flight Mechanics Design," 2012. https://doi.org/10.2514/6.2012-5966.

[14] Guadagnini, J., De Zaiacomo, G., and Bussler, L., "Aerodynamic Coefficients Estimation Tool for re-entry Vehicle Missionisation," *2nd International Conference on Flight Vehicles Aerothermodynamics and Re-entry Missions and Engineering (FAR)*, 2022.

[15] Haya Ramos, R., Penin, L., Parigini, C., Kerr, M., Preaud, J.-P., Ganet, M., Bennani, S., and Martinez Barrio, A., "Flying Qualities Analysis for Re-entry Vehicles: Methodology and Application," 2011. https://doi.org/10.2514/6.2011-6344.

[16] Mooij, E., "Re-entry Systems, Lecture Notes," , 2015.

[17] Sagliano, M., and Mooij, E., "Optimal drag-energy entry guidance via pseudospectral convex optimization," *Aerospace Science and Technology*, Vol. 117, 2021, p. 106946.

[18] Saraf, A., Leavitt, J., Ferch, M., and Mease, K., "Landing footprint computation for entry vehicles," *AIAA Guidance, Navigation, and Control Conference and Exhibit*, 2004, p. 4774.

[19] NATIONAL OCEANIC AND ATMOSPHERIC ADMINISTRATION ROCKVILLE MD, "U.S. Standard Atmosphere, 1976," 1976.

[20] Saraf, A., Leavitt, J., Chen, D., and Mease, K., "Design and evaluation of an acceleration guidance algorithm for entry," *Journal of Spacecraft and Rockets*, Vol. 41, No. 6, 2004, pp. 986–996.

[21] Betts, J. T., "Survey of numerical methods for trajectory optimization," *Journal of guidance, control, and dynamics*, Vol. 21, No. 2, 1998, pp. 193–207.

[22] Betts, J. T., *Practical methods for optimal control and estimation using nonlinear programming*, SIAM, 2010.

[23] Murray, W., "Sequential quadratic programming methods for large-scale problems," *Computational Optimization and Applications*, Vol. 7, No. 1, 1997, pp. 127–142.

[24] Chachuat, B., "Nonlinear and dynamic optimization: From theory to practice," Tech. rep., 2007.

[25] Liu, X., Shen, Z., and Lu, P., "Solving the Maximum-Crossrange Problem via Successive Second-Order Cone Programming with a Line Search," *Aerospace Science and Technology*, Vol. 47, 2015. https://doi.org/10.1016/j.ast.2015.09.008.

[26] Martins, J. R., and Lambe, A. B., "Multidisciplinary design optimization: a survey of architectures," *AIAA journal*, Vol. 51, No. 9, 2013, pp. 2049–2075.

[27] Balesdent, M., Bérend, N., Dépincé, P., and Chriette, A., "A survey of multidisciplinary design optimization methods in launch vehicle design," *Structural and Multidisciplinary optimization*, Vol. 45, No. 5, 2012, pp. 619–642.

[28] Gray, J. S., Hwang, J. T., Martins, J. R. R. A., Moore, K. T., and Naylor, B. A., "OpenMDAO: An open-source framework for multidisciplinary design, analysis, and optimization," *Structural and Multidisciplinary Optimization*, Vol. 59, No. 4, 2019, pp. 1075–1104. https://doi.org/10.1007/s00158-019-02211-z.